Analysis of Self-Pulsating Sources Based on Cascaded Regeneration and Soliton Self-Frequency Shifting

Thibault North, Alaa Al-kadry, and Martin Rochette

***Abstract*—We characterize the operation of self-pulsating sources made of two optical regenerators in cascade, namely a first regenerator of the type self-phase modulation spectral broadening and offset filtering, followed by a second regenerator of the type supercontinuum generation and offset filtering. The range of operation of this laser is explored as the wavelength and bandwidths of the band-pass filters are adjusted. We also provide experimental evidence that soliton self-frequency shift emanating from modulation instability triggers bursts of pulses at the repetition rate of the cavity. The stochastic nature of sources based on this concept leads to shot-to-shot pulse fluctuations in the cavity, which on average result in a flat supercontinuum extending beyond 1900 nm. Finally, a seed pulse can be sustained efficiently via this laser architecture, and the cavity consequently generates subpicosecond pulses at one of its output.**

***Index Terms*—Self-pulsating source, laser resonator, nonlinear optics, self-phase modulation, optical pulse regeneration, soliton self-frequency shifting, modulation instability.**

I. Introduction

SELF-pulsating fiber lasers have become a topic of interest for their ability to combine a high beam quality, stability and compactness. In such lasers, the generation of short pulses enables imaging, spectroscopy or metrology as well as industrial application when operating at watt levels [1]. To generate pulses, a nonlinear transfer function favoring pulses over continuous wave (CW) operation must be added in the laser cavity. Within the category of pulsed lasers that are all-fiber, mode-locking with nonlinear polarization rotation [2] or nonlinear loop mirrors [3], [4] are the most common ways to generate ultrashort pulses of large bandwidths.

In 2008, pulsed lasers based on a pair of complementary regenerators of type self-phase modulation (SPM) and offset filtering (SPM-OF) regenerators was demonstrated [5]. This architecture has interesting features including aperiodicity, low polarization sensitivity, and multiwavelength operation [6]–[8]. Pulses propagating in sources based on that concept undergo large changes in their spectral and temporal profile twice per cavity round trip. As a result, their output feature invariant eigenpulses which can be regarded as dispersion-managed solitons [9]. These sources do not belong to the class of mode-locked lasers, for which a fixed phase relationship is maintained between the spectral components of the propagating beam. Consequently, the repetition rate of the output pulses is not constrained to a pulse-to-pulse time interval dictated by the cavity free spectral range or one of its harmonics.

Based on cascaded regeneration, a new method for generating short pulses in fiber lasers was also proposed and demonstrated experimentally in 2012 [10]. Sources of that kind, referred to as SPM-soliton self-frequency shift (SPM-SSFS) sources, are composed of two distinct regeneration stages. In the first stage, regeneration based on SPM-OF is followed by a second regeneration stage in which SSFS occurs during the generation of a supercontinuum (SC). This SC is partially washed out by a red-shifted band-pass filtering (BPF), and the ring cavity is closed as the output of the second stage becomes the input of the first stage. Hence, the design of SPM-SSFS sources has similarities with self-pulsating sources based on cascaded SPM-OF regenerators, which also feature wavelength toggling and alternating offset filtering. A particular feature of SPM-SSFS sources is that they provide a broadband SC at one of their output, along with a tunable temporal burst duration which can be extended up to several hundreds of nanoseconds when the pump power is increased. Because of the presence of multiple and varying pump pulses, the SC generated by this type of sources may be compared to supercontinua emanating from noise bursts [11], [12] or noiselike pulses [13]. SPM-SSFS sources therefore provide a flexible platform for ultrashort pulse generation, which results in a tunable output energy and SC width, without active optical elements such as optical modulators. Moreover, no saturable absorber is required to trigger and sustain the pulsed regime, which enables compact and robust all-fiber setups. Overall, SPM-SSFS sources compose an interesting new architecture, which so far has not been the subject of much investigation. In [10], numerical simulations were provided along with spectral measurements to support the possibility that a pulse originating from the first nonlinear stage is turned into several fundamental solitons, shifted in frequency by stimulated Raman scattering (SRS) during propagation in the anomalous dispersion region of a highly nonlinear fiber (HNLF). However, multishot spectral measurements have provided an averaged spectrum rather than a direct experimental observation of this process.

Manuscript received November 22, 2013; revised March 19, 2014; accepted March 21, 2014. This work was supported by the National Optics Institute (INO) in Quebec City, QC, Canada.

The authors are with the Department of Electrical and Computer Engineering, McGill University, Montréal, QC H3A 2A7, Canada (e-mail: thibault.north@mail.mcgill.ca; alaa.al-kadry@mail.mcgill.ca; martin.rochette@mcgill.ca).

Color versions of one or more of the figures in this paper are available online at http://ieeexplore.ieee.org.

Digital Object Identifier 10.1109/JSTQE.2014.2313913

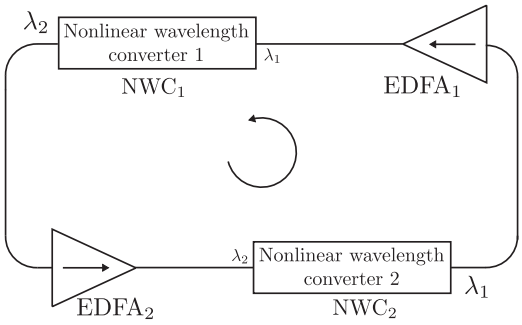

Fig. 1. Setup of a generic self-pulsating source based on cascaded regeneration. EDFA: erbium-doped fiber amplifier.

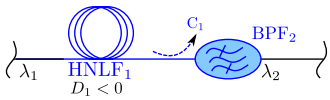

Fig. 2. First nonlinear stage: SPM-OF regenerator. BPF: band-pass filter, HNLF: highly nonlinear fiber.

In this paper, we experimentally investigate the conditions for pulse ignition and SC generation from the influence of filters in the cavity. Results provide the optimal filter bandwidth that maximizes the output SC bandwidth as well as the total output power. Shot-to-shot spectral measurements indicate, as previously assumed in [10], that the observed SC originates from the time-averaging of multiple spectra. These SCs, seeded by picosecond pulses, are extremely sensitive to initial conditions, and therefore their output spectra are unique [14]. Finally, numerical simulations are conducted, and show that the architecture of SPM-SSFS sources can sustain pulses in a SC-free regime, by avoiding the generation of multiple solitons. In this case, the source efficiency is maximal, and subpicosecond pulses are readily available at one cavity output.

II. Theoretical Basis and Experimental Setup

Self-pulsating sources based on cascaded regeneration rely on two or more nonlinear stages whose function is to convert the propagating signal from one wavelength to another. When there are two nonlinear stages, the initial signal is shifted from the wavelength $\lambda_{1,2}$ to the wavelength $\lambda_{2,1}$ via nonlinear wavelength converters (NWCs), as depicted in Fig. 1. These NWCs must feature intensity dependent transfer functions and hence favor high intensities, triggering pulses. Regenerative sources solely composed of cascaded SPM-OF regenerators at $\mathrm{NWC}_{1,2}$ sustain pulses with a low amplitude jitter, due to the sharp transfer function that characterizes the SPM-OF regenerators placed in the cavity [6]. The temporal shape of the pulses is imposed by the spectral shape of the filters, via their Fourier transform plus an additional chirp, linear across the pulse. Fig. 2 depicts such a regenerator. In fact, a remarkable property of SPM-OF regenerators is that at the first approximation, the output pulse peak power is independent of the input pulse power. Given that the latter is above threshold, the output peak power P_ω is expressed as [15]:

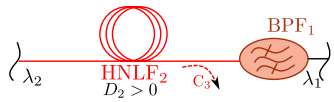

Fig. 3. Second nonlinear stage: SSFS induced by MI and followed by selective filtering. BPF: band-pass filter, HNLF: highly nonlinear fiber.

$$P_\omega \sim \frac{P_p}{\Delta\omega_{\mathrm{SPM}}} = \frac{1}{\lambda}\Delta\omega_0 2\pi n_2 L. \tag{1}$$

In equation (1), the output intensity is proportional only to the initial bandwidth ω_0, as well as the nonlinear propagation length L and the nonlinear coefficient n_2. The central wavelength is λ, $\Delta\omega_0$ is the input pulse bandwidth, $\Delta\omega_{\mathrm{SPM}}$ is the bandwidth of the pulses broadened by SPM, and P_p is the input pulse peak power. Amplitude variations are, therefore, limited by this first nonlinear stage, which generates nearly chirp-free pulses at its output at small filter bandwidths, and linearly chirped pulses at larger spectral filter bandwidths [7].

In SPM-SSFS sources, the second NWC (NWC_2) is a HNLF with anomalous dispersion at the pump wavelength used in tandem with a BPF, as depicted in Fig. 3. Pulses input to this NWC undergo SSFS, induced by modulation instability (MI) when their temporal duration is in the picosecond range [16]. By joining both nonlinear stages with EDFAs, the source self-ignites pulses from amplified spontaneous emission (ASE), provided that the BPFs have an adequate relative spectral position, which is the subject of Section III.

Fig. 4 depicts the experimental setup used in this work. This setup has similarities with the setup of Ref. [10], Fig. 1, but is improved with the use of tunable and adjustable filters for both BPF_1 and BPF_2, replacing the fixed filter formed by the conjunction of an optical circulator and a Bragg grating, thereby adding two degrees of freedom. This setup is composed of two HNLFs of length $L = 1007$ m, two adjustable and tunable BPFs, centered at the wavelengths $\lambda_{1,2}$, and with tunable 3 dB bandwidths $\Omega_{1,2}$, respectively. The filters have sharp edges, as shown in Fig. 4(d), and a modification of their bandwidth only alters the width of their flat top portion. The filter offset is defined as $\Delta\lambda = |\lambda_1 - \lambda_2|$. The nonlinear fibers $\mathrm{HNLF}_{1,2}$ have a nonlinear waveguide coefficient $\gamma = 12.5\ \mathrm{W}^{-1}\cdot\mathrm{km}^{-1}$, and a chromatic dispersion coefficient $D_1 = -0.71$ ps/(nm·km) and $D_2 = 2.09$ ps/(nm·km), respectively. Their third-order dispersion coefficients are $S_1 = 0.0074$ ps/(nm^2·km) and $S_2 = 0.002$ ps/(nm^2·km). Insertion losses are of 1.7 dB for each HNLF, 8 dB for BPF_1, 5.5 dB for BPF_2, and 0.5 dB for each output coupler, in addition to the power drawn by their output port. Two EDFAs are inserted between each nonlinear stage, with a saturation power $P_{\mathrm{sat}} \approx 15$ dBm. The cavity output is observed via the four output tap couplers C_{1-4} with a 12.5 GHz photodiode and a standard optical spectrum analyzer (OSA). The 1% tap couplers are used for monitoring purposes. The extraction of 10% of the cavity power at C_1 and C_3 is sufficient to obtain output powers up to 10 dBm. The EDFAs are used below 50% of their capacity in terms of pump power, and higher coupling ratios could be used without altering the source operation.

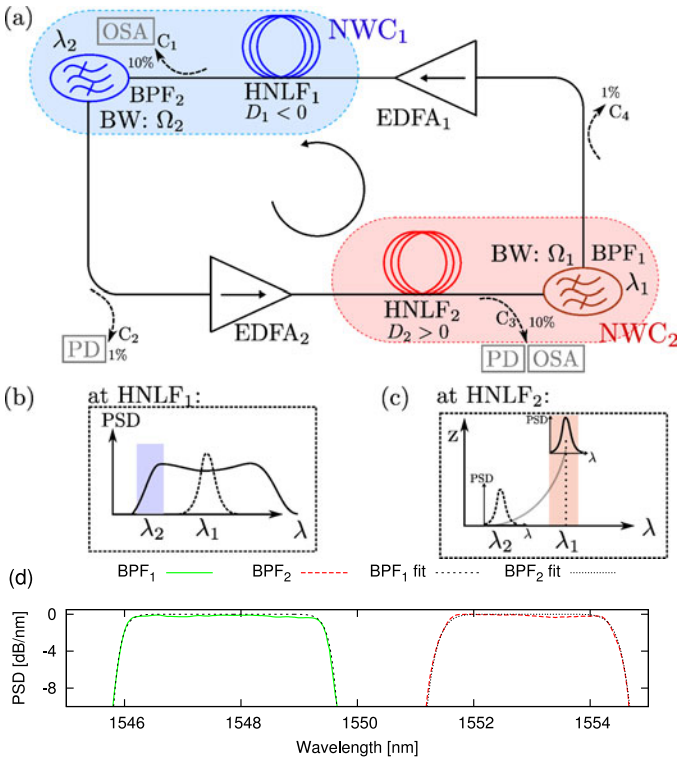

Fig. 4. Closed-loop self-pulsating cavity. (a) Experimental setup of the SPM-SSFS source. (b) spectrum at the first nonlinear stage, with SPM broadening and offset filtering at λ_2. (c) SSFS and filtering at λ_1, in the second nonlinear stage, (d) Illustration of the filter profiles. BPF: band-pass filter, BW: bandwidth, HNLF: highly nonlinear fiber, EDFA: erbium-doped fiber amplifier, NWC: nonlinear wavelength converter, OSA: optical spectrum analyzer, PD: photodiode, PSD: power spectral density.

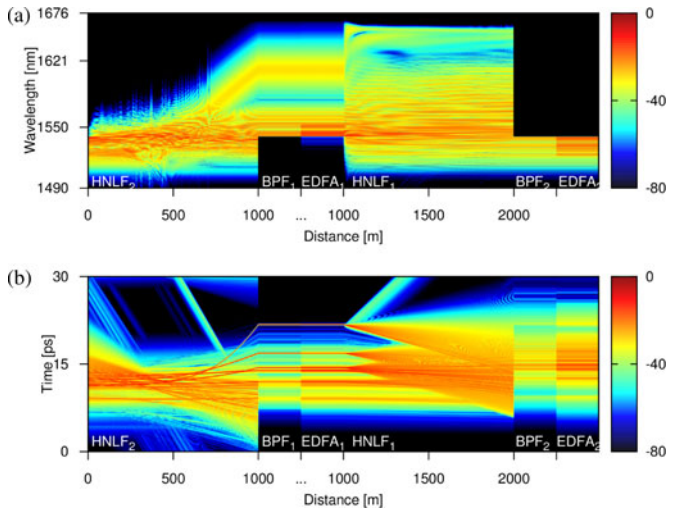

Fig. 5. Propagation of pulses in the cavity of Fig. 4(a). (a) In the frequency domain and (b) in the time domain. The propagation length of the BPFs and EDFAs are increased for readability.

In Fig. 5, the propagation of pulses is shown in the spectral and temporal domain after 18 cavity round-trips. The limit case where BPF_1 is a low-pass filter and BPF_2 is a high-pass filter is illustrated. Pulses from $EDFA_2$ are launched into $HNLF_2$, and interact by the conjugated effects of MI and four-wave mixing (FWM). These interactions give birth to fundamental solitons, which experience SSFS as illustrated in Fig. 5(a), where a powerful soliton shifts to a wavelength of ~ 1630 nm. In the time domain, these solitons acquire a delay because of their different group-velocity in the anomalous dispersion regime. Dispersive waves are also emitted as a result of these interactions, and the observed spectrum is similar to spectra arising from supercontinua seeded by picosecond pulses. Solitons resulting of the propagation in $HNLF_2$ experience a significant amount of SPM when propagating in $HNLF_1$. This results in a large temporal broadening, as well as a weak emission of radiation from the blue-most wavelength components of these pulses, which now propagate slower than red-most wavelength components in normal dispersion. Low-pass filtering at BPF_1 do not extinct the significantly shifted solitons. However, they do not benefit from the gain of $EDFA_1$, nor pass through BPF_2. For other spectral components, SPM broadening occurs in the first few meters of the fiber, thereby shifting some energy towards the shorter wavelengths and resetting the central wavelength to λ_2, as depicted in Fig. 4(b). The numerical model used to generate Fig. 5 includes the effects of second- and third-order dispersion $\beta_{2,3}$, nonlinearities, and the Raman effect ($T_R = 3$fs), and is implemented as described in [8].

III. Effect of the Filter Bandwidths

The output properties of SPM-SSFS sources were studied in [10] for fixed filter spectral positions and bandwidths. The source was started from ASE, as the pump power of $EDFA_{1,2}$ was increased beyond a given power threshold. In this section, the operation of the source is shown for a wide range of filter spectral bandwidths, and pulses are triggered by altering the filter offset. At one limiting case, BPF_1 is a low-pass filter, and BPF_2 is a high-pass filter. Experimentally, this case is implemented by maximizing the bandwidth of the filters, so that they exceed the erbium gain window. At the opposite limiting case, both BPFs have a narrow bandwidth < 0.5 nm, and the source operates in a CW regime, with amplified fluctuations induced by MI. In this configuration, the propagation in $HNLF_2$ is comparable to the self-pulsating laser introduced by Lee *et al.* [17] which generates a broadband SC from MI in a ring cavity, except for the fact that the pump power is two orders of magnitude lower than the one reported in [17].

In Fig. 6, BPF_1 is a low-pass filter, and BPF_2 has a variable bandwidth. Self-pulsation occurs for a fixed EDFA pump power, by reducing the spectral separation between the BPFs, by red-shifting BPF_2. The green zone of Fig. 6(a) represents the maximal filter offset that induces self-pulsation. This zone has a maximal $\Delta\lambda$ when $\Omega_2 = 3$ nm. Fig. 6(b) illustrates the continuum observed at C_3 for some of these configurations. For a BPF_2 bandwidth of 3.5 nm, the continuum generated at C_3 is maximized, and reaches wavelengths past 1900 nm. For larger and smaller bandwidths, less energy is transferred towards the long wavelengths. Hence, there exist an optimal spectral bandwidth of BPF_2 for which the captured spectral power density contributes optimally to sustain the existing pulses in the cavity. This particular case was illustrated in [18], in the case of

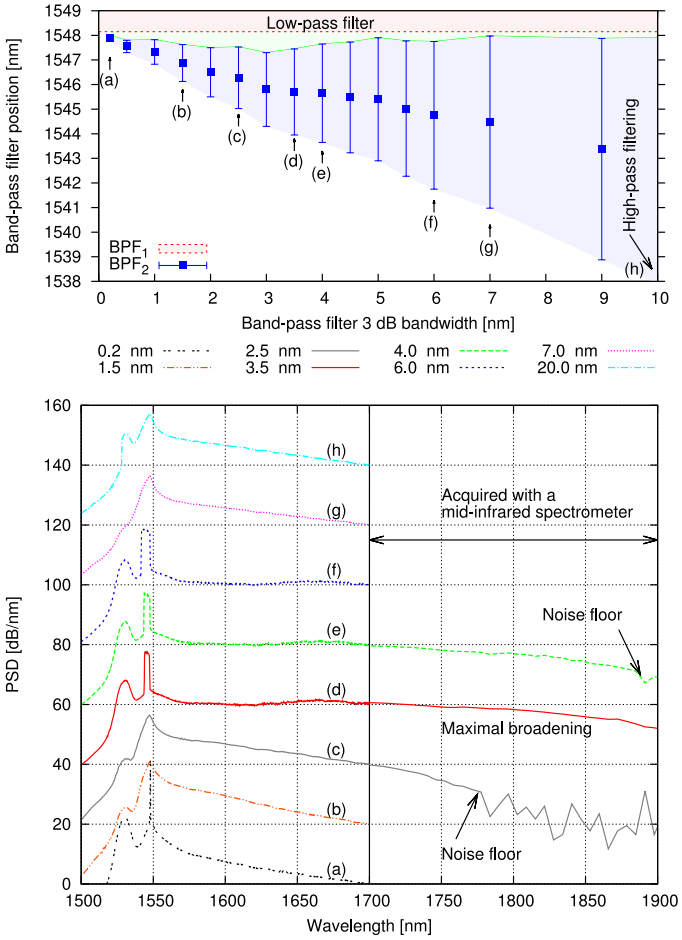

Fig. 6. (a) Filter position for variable bandwidths of BPF_2. The spectral position of BPF_2 corresponds to the blue-most position which triggers pulses in the cavity. (b) Spectrum at output C_3 for different values of bandwidth of BPF_2. The leftmost part of the graph is acquired with a standard OSA, while the rightmost part of the graph is acquired with a NearQuest spectrometer of lower dynamic range, operating in the range 1000–2400 nm.

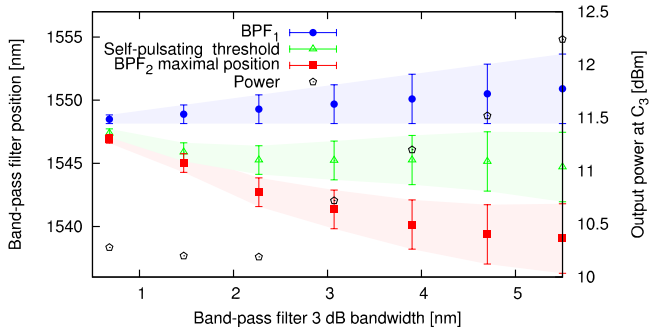

Fig. 7. Operation of the SPM-SSFS source at several different filter bandwidths. The error bars represent the 3 dB bandwidth of the filters. The self-pulsating threshold position is depicted as well as the maximal spectral shift of BPF_2 that is reached without altering the source operation. The output power corresponding to the threshold is reported on the right axis.

regenerative sources. In such a situation, the pulses filtered at BPF_2 exhibit long temporal duration due to the accumulated dispersion, or contain a broad pedestal if compression is achieved by chirp compensation. The pulse energy is high due to the large amount of spectral components captured by the BPF, but it is spread over a long duration, which is nonoptimal for SC generation.

In a second set of experiments, the filter bandwidths are changed, so that $\Omega_1 = \Omega_2$ at all times. In Fig. 7, the position of each BPF is depicted. BPF_2 is first shifted towards the longer wavelengths to trigger self-pulsation, and the output power at C_3 is recorded at that moment. Then, BPF_2 is shifted in the opposite direction, and the wavelength at which the source stops pulsating is recorded. For filter bandwidths of 4.7 nm, pulses are sustained in the cavity up to a filter offset of $\Delta\lambda = 3$ nm. Spectrally, the continuum at C_3 shows insignificant changing when altering the filters bandwidth. Even for filter bandwidths of 0.5 nm, which means large temporal pulse duration of $\sim$7 ps from the SPM-OF regenerator, SC generation is initiated in $HNLF_2$.

Overall, SPM-SSFS sources self-start from thin filter bandwidths of 0.5 nm to ultra-large bandwidths in the limiting case, when reduced to a pair of low- and high-pass filters. Optimal filter bandwidths maximize the source efficiency by blocking the spectral content which does not contribute to the pulses.

IV. Single-Shot Spectral Measurements

A wavelength-to-time mapping technique is used to capture the power spectral density of pulses originating from $HNLF_2$ [19]. Used recently to analyze supercontinua induced by MI or noiselike pulses [20], [21], this technique relies on the fact that any pulse tends to turn into its Fourier transform when passing through a dispersive medium. When the third-order dispersion is small, the last term of Eq. (2) is negligible, and Eq. (2) provides a linear relationship between a time interval $\Delta\tau$, a wavelength interval $\Delta\lambda$, the chromatic dispersion coefficient D and the fiber length L [19]

$$\Delta\tau \approx DL\Delta\lambda + \frac{\mathrm{d}}{\mathrm{d}\lambda}DL(\Delta\lambda^2). \tag{2}$$

A spool of 21.64 km of SMF-28, for which this assumption holds, is used along with a real-time oscilloscope. The temporal duration of the observed signal must be small with respect to the time-delay corresponding to the signal bandwidth. Because SPM-SSFS sources generate a burst of pulses at their output, it is necessary to reduce the burst duration to a minimal value. For this purpose, the EDFA pump power is decreased to shorten the duration of the temporal burst after the regeneration stage. Fig. 8 presents a set of unrelated 30 single-shot spectra, when BPF_1 and BPF_2 have a bandwidth of 5 nm and 6 nm, respectively. This set of spectra reveals several peaks at various wavelengths, red-shifted with respect to the pump, which correspond to powerful solitons shifted by SRS. Fig 5(a) indicates that co-propagating solitons exchange energy as they collide with others [22]–[24]. The soliton temporal duration can be retrieved from their bandwidth at the output C_3. From the solitons of Fig. 8(a) whose full width at half maximum (FWHM) is separated from other spectral components, the soliton temporal FWHM are of $\sim$120 fs – 200 fs, for a spectral bandwidth of 12–21 nm. As

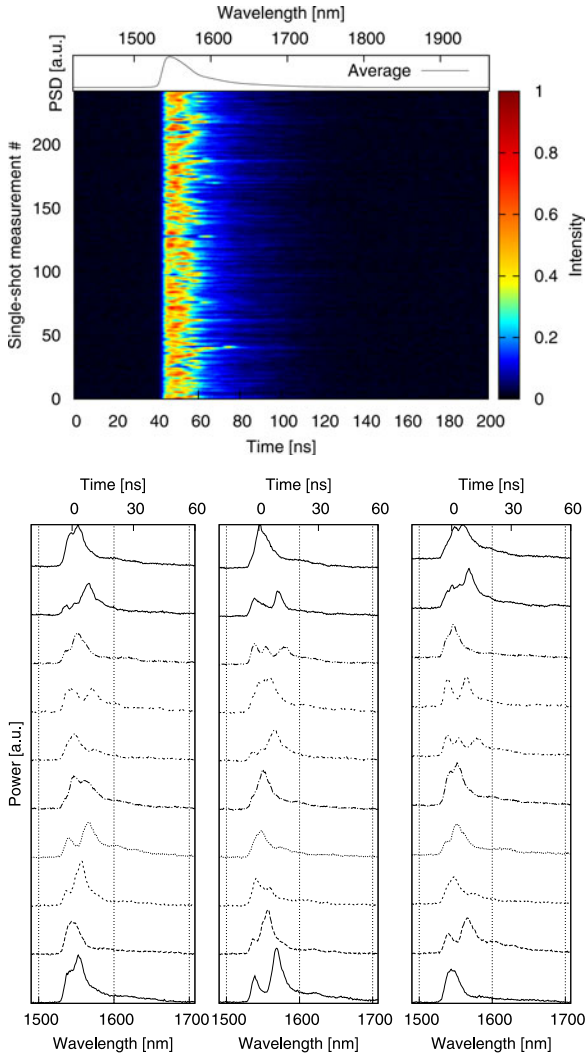

Fig. 8. (a) Single-shot measurements of the spectrum at C_3. (b) Spectra corresponding to 30 independent single-shot measurements of (a).

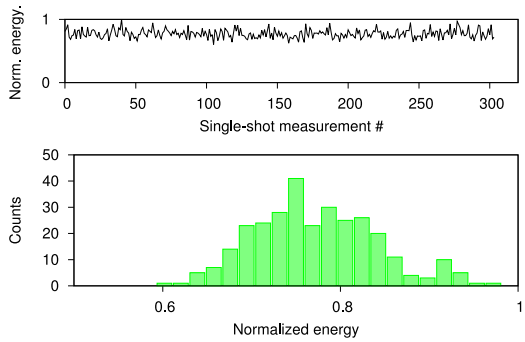

Fig. 9. Energy retrieved from single-shot measurements, integrated from the time-domain spectral measurements.

indicated by Fig. 8(a), a small amount of energy is nevertheless transferred to the longer wavelengths, up to 1700 nm, revealing the presence of solitons of short temporal duration whose frequency shift is proportional to $1/t_{\mathrm{twhm}}^4$ [25]. The shifting rate is also potentially raised by collisions with other solitons generated by MI [24]. The randomness characteristics of SC generation induced by MI imply that the energy contained in the cavity is not constant, contrary to mode-locked lasers or sources based solely on cascaded SPM-OF regenerators. The offset filtering periodically reduces the number of pulses, and the total pulse energy varies as depicted in Fig. 9.

V. SC-Free Operation

In this section, we numerically investigate the potential of SPM-SSFS sources for SC-free operation, a regime in which a single pulse propagates in the cavity with a minimum energy loss. The operation of SPM-SSFS sources according to the setup of Fig. 4 is such that the pulse input to HNLF_2 is chirped, in the picosecond range, and energetic. This pulse is split into several fundamental solitons, drifting with various amounts of spectral shifts. Most of the time, these solitons are therefore rejected by BPF_1. If BPF_1 is a low-pass filter, the solitons are sustained in HNLF_1 but rejected at BPF_2, because their spectral broadening by SPM is insufficient to transfer energy back to λ_2. In this case, the source efficiency is limited as illustrated by the SC observed at C_3.

However, are SPM-SSFS sources able to generate and sustain a single pulse, which could undergo SSFS and transfer most of the energy from the short towards the long wavelengths? To answer this question, the setup of Fig. 4 is altered by the addition of a dispersion compensating fiber after EDFA_2. Chirp compensation therefore decreases the pulse input to HNLF_2 down to a FWHM duration of 300 fs. At such pulse duration, propagation in HNLF_2 enables SSFS of a single soliton, because the effects of MI and FWM do not prevail [26].

Simulations conducted with various filter bandwidths, gain and saturation indicate that single-pulse operation is supported by the cavity. However, the source is not self-starting in this configuration. To trigger pulses, the required saturation energy leads to higher order solitons of $N > 2$ input to HNLF_2, contradicting the requirement for single-pulse operation. Nevertheless, if a pulse seed is launched in a cavity with adequate amplifiers, the SPM-SSFS source reaches a steady-state, sustaining picosecond pulses in HNLF_1, and subpicosecond in HNLF_2. Fig. 10 illustrates the steady-state propagation of a single pulse inside the cavity, in the time and frequency domains, after 10 cavity round-trips. The BPFs are Gaussian, with a FWHM bandwidth of 5 nm, and their spectral separation $\Delta\lambda = 10$ nm. The saturation power of $\mathrm{EDFA}_{1,2}$ are of 0.075 and 2.11 dBm, respectively. A length of 42 m of single-mode fiber compensates for the dispersion in HNLF_1. In this configuration, 37% of the power input to HNLF_2 passes through BPF_1. The SPM-OF regenerator is less efficient, and passes 14% of the resulting power. The experimental design of a cavity enabling SC-free operation would require a proper tuning of the doped-fiber lengths. The initial pulse can be seeded at C_2, and monitored at C_4 and C_1. By adjusting the pump power of the EDFAs, the required spectral shift which maximizes transmission can be reached at each nonlinear stage.

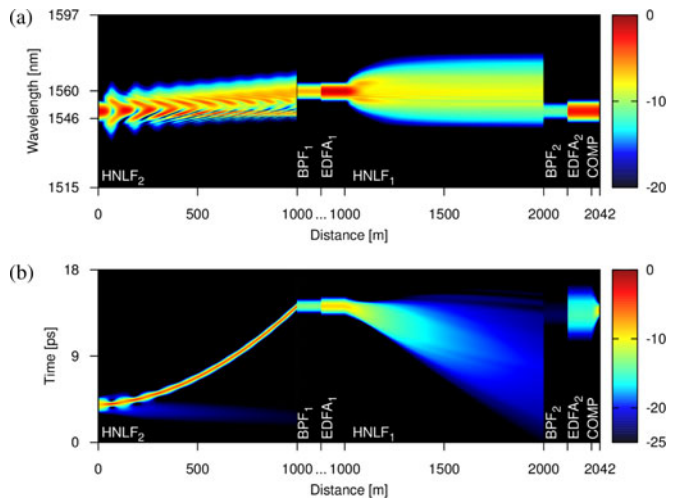

Fig. 10. Propagation of a single pulse in the cavity. (a) In the frequency domain and (b) in the time domain. The propagation length of the BPFs and EDFAs are increased for readability.

VI. Conclusion

The operation of self-pulsating sources based on SPM-OF regenerators as well as SSFS followed by offset filtering is characterized temporally and spectrally. The range of operation of this cavity is broader than the one observed previously. The bandwidth of BPF_2 has a direct influence on the width of the SC generated at C_3. An optimal filter bandwidth of 3.5 nm leads to a broad SC, which extends past 1900 nm, and potentially further with the use of a HNLF pumped closer to the zero-dispersion wavelength than the one currently used. A spectrally narrow BPF_2, on the other hand, leads to an operation regime close to the one of CW SC sources. The experimental setup of this source could be further simplified at the expense of a maximized output continuum by replacing the BPFs with low- and high-pass filters.

Single-shot measurements illustrate that the mechanism of pulse generation in $HNLF_2$ is induced by MI and FWM. This process is stochastic, and the SC produced at C_3 is the time-average of several solitons, shifted by SRS. The source itself hence exhibits a stochastic behavior, and the energy sustained in the cavity is time-dependent, contrary to mode-locked lasers with output pulses of constant energy. SPM-SSFS sources have a simple yet efficient architecture for broadband light generation. In the absence of bulk saturable absorber, their operation at other central wavelength is readily conceivable, and the source does not require complex alignment or polarization tweaking. The generation of light over a large bandwidth makes SPM-SSFS sources a candidate for applications in spectroscopy, and its intrinsic stochastic behavior may find applications in random number generation, as well as chaotic LIDARs and imaging. We expect that this architecture would also operate at different wavelengths using appropriate gain media such as e.g. other rare-earth doped glasses or nonlinear gain, permitting light generation in the mid-infrared via SC generation at C_3.

Finally, simulations indicate that SC-free operation can be sustained in SPM-SSFS sources, provided that a pulse seed is input to the cavity.

Acknowledgment

The authors are thankful to Pierre Galarneau (INO) for insightful discussions, and acknowledge the help of K. Ramaswamy for the data acquisition.

References

[1] W. Sibbett, A. A. Lagatsky, and C. T. A. Brown, "The development and application of femtosecond laser systems," *Opt. Exp.*, vol. 20, no. 7, pp. 6989–7001, Mar. 2012.
[2] K. Sala, M. Richardson, and N. R. Isenor, "Passive mode locking of lasers with the optical Kerr effect modulator," *IEEE J. Quantum Electron.*, vol. QE-13, no. 11, pp. 915–924, Nov. 1977.
[3] N. J. Doran and D. Wood, "Nonlinear-optical loop mirror," *Opt. Lett.*, vol. 13, no. 1, pp. 56–58, Jan. 1988.
[4] M. E. Fermann, F. Haberl, M. Hofer, and H. Hochreiter, "Nonlinear amplifying loop mirror," *Opt. Lett.*, vol. 15, no. 13, pp. 752–754, Jul. 1990.
[5] M. Rochette, L. R. Chen, K. Sun, and J. Hernandez-Cordero, "Multiwavelength and tunable self-pulsating fiber cavity based on regenerative SPM spectral broadening and filtering," *IEEE Photon. Technol. Lett.*, vol. 20, no. 17, pp. 1497–1499, Sep. 2008.
[6] S. Pitois, C. Finot, L. Provost, and D. J. Richardson, "Generation of localized pulses from incoherent wave in optical fiber lines made of concatenated Mamyshev regenerators," *J. Opt. Soc. Amer. B*, vol. 25, no. 9, pp. 1537–1547, 2008.
[7] K. Sun, M. Rochette, and L. R. Chen, "Output characterization of a self-pulsating and aperiodic optical fiber source based on cascaded regeneration," *Opt. Exp.*, vol. 17, no. 12, pp. 10419–10432, Jun. 2009.
[8] T. North and M. Rochette, "Analysis of Self-pulsating sources based on regenerative SPM: Ignition, pulse characteristics and stability," *J. Lightw. Technol.*, vol. 31, no. 23, pp. 3700–3706, Dec. 2013.
[9] S. K. Turitsyn, B. G. Bale, and M. P. Fedoruk, "Dispersion-managed solitons in fibre systems and lasers," *Phys. Rep.*, vol. 521, no. 4, pp. 135–203, Dec. 2012.
[10] T. North and M. Rochette, "Broadband self-pulsating fiber laser based on soliton self-frequency shift and regenerative self-phase modulation," *Opt. Lett.*, vol. 37, no. 14, pp. 2799–2801, Jul. 2012.
[11] J. W. Nicholson, A. K. Abeeluck, C. Headley, M. F. Yan, and C. G. Jørgensen, "Pulsed and continuous-wave supercontinuum generation in highly nonlinear, dispersion-shifted fibers," *Appl. Phys. B*, vol. 77, no. 2-3, pp. 211–218, Sep. 2013.
[12] Y. Takushima, "High average power, depolarized supercontinuum generation using a 1.55-μm ASE noise source," *Opt. Exp.*, vol. 13, no. 15, pp. 5871–5877, Jul. 2005.
[13] J. C. Hernandez-Garcia, O. Pottiez, J. M. Estudillo-Ayala, and R. Rojas-Laguna, "Numerical analysis of a broadband spectrum generated in a standard fiber by noise-like pulses from a passively mode-locked fiber laser," *Opt. Commun.*, vol. 285, no. 7, pp. 1915–1919, Apr. 2012.
[14] D. R. Solli, C. Ropers, P. Koonath, and B. Jalali, "Optical rogue waves," *Nature*, vol. 450, no. 7172, pp. 1054–1057, 2007.
[15] P. Mamyshev, "All-optical data regeneration based on self-phase modulation effect," in *Proc. IEEE 24th Eur. Conf. Opt. Commun.*, vol. 1, 1998, pp. 475–476.
[16] G. P. Agrawal. (2007). *Nonlinear Fiber Optics* (ser. Optics and Photonics). New York, NY, USA: Academic [Online]. Available: http://books.google.ca/books?id=UaY1MLmC780C
[17] J. Lee, Y. Takushima, and K. Kikuchi, "Continuous-wave supercontinuum laser based on an erbium-doped fiber ring cavity incorporating a highly nonlinear optical fiber," *Opt. Lett.*, vol. 30, no. 19, pp. 2599–2601, 2005.
[18] T. North and M. Rochette, "Regenerative self-pulsating sources of large bandwidths," *Opt. Lett.*, vol. 39, no. 1, pp. 174–177, Jan. 2014.
[19] P. Kelkar, F. Coppinger, A. S. Bhushan, and B. Jalali, "Time-domain optical sensing," *Electron. Lett.*, vol. 35, no. 19, pp. 1661–1662, 1999.
[20] B. Wetzel, A. Stefani, L. Larger, P. A. Lacourt, J. M. Merolla, T. Sylvestre, A. Kudlinski, A. Mussot, G. Genty, F. Dias, and J. M. Dudley, "Real-time full bandwidth measurement of spectral noise in supercontinuum generation," *Sci. Rep.*, vol. 2, 2012.

[21] A. F. J. Runge, C. Aguergaray, N. G. R. Broderick, and M. Erkintalo, "Coherence and shot-to-shot spectral fluctuations in noise-like ultrafast fiber lasers," *Opt. Lett.*, vol. 38, no. 21, pp. 4327–4330, Nov. 2013.
[22] S. Chi and S. Wen, "Raman cross talk of soliton collision in a lossless fiber," *Opt. Lett.*, vol. 14, no. 21, pp. 1216–1218, Nov. 1989.
[23] M. N. Islam, G. Sucha, I. Bar-Joseph, M. Wegener, J. P. Gordon, and D. S. Chemla, "Femtosecond distributed soliton spectrum in fibers," *J. Opt. Soc. Amer. B*, vol. 6, no. 6, pp. 1149–1158, Jun. 1989.
[24] M. H. Frosz, O. Bang, and A. Bjarklev, "Soliton collision and Raman gain regimes in continuous-wave pumped supercontinuum generation," *Opt. Exp.*, vol. 14, no. 20, pp. 9391–9407, Oct. 2006.
[25] J. Gordon, "Theory of the soliton self-frequency shift," *Opt. Lett.*, vol. 11, no. 10, pp. 662–664, 1986.
[26] J. M. Dudley, G. Genty, and S. Coen, "Supercontinuum generation in photonic crystal fiber," *Rev. Mod. Phys.*, vol. 78, pp. 1135–1184, Oct. 2006.

Thibault North received the M.Sc. degree in engineering from the University of Applied Sciences and Arts, Western Switzerland, Delémont, Switzerland, in 2011. He is working toward the Ph.D. degree at the Photonic Systems Group at McGill University, Montréal, QC, Canada.

Alaa Al-kadry received the M.Sc. degree in physics from the University of Waterloo, Waterloo, ON, Canada, in 2010. He is currently working toward the Ph.D. degree in electrical and computer engineering at McGill University, Montréal, QC, Canada. His current research focuses on the development of broadband and midinfrared sources.

Martin Rochette is an Associate Professor with the Department of Electrical and Computer Engineering, McGill University, Montréal, QC, Canada. He has authored or coauthored more than 135 journal and conference papers on highly nonlinear materials and devices, fiber laser sources, optical fiber components, and optical communication systems. His current research interests include the application of nonlinear effects for devices and laser sources with applications for biomedicine, instrumentation, and telecommunication systems.